

# Sol–gel synthesis, crystal structure, surface morphology, and optical properties of $\text{Eu}_2\text{O}_3$ -doped $\text{La}_2\text{Mo}_3\text{O}_{12}$ ceramic

Ruta Stankeviciute · Arturas Zalga

Received: 31 October 2013 / Accepted: 20 May 2014 / Published online: 18 June 2014  
© Akadémiai Kiadó, Budapest, Hungary 2014

**Abstract** In this paper, we report the synthesis of the La–Mo–O tartrate gel precursors with the initial composition for  $\text{La}_2\text{Mo}_3\text{O}_{12}$  ceramic prepared from different starting materials by an aqueous sol–gel synthesis route using tartaric acid as a complexing agent. Moreover, the La–Mo–O carbonate–tartrate and nitrate–tartrate gel precursors doped with  $x$  % of  $\text{Eu}_2\text{O}_3$  ( $x = 0.5, 1.0, 2.0, 4.0,$  and  $8.0$ ) by aqueous sol–gel synthesis method were also prepared. The thermal decomposition of both the La–Mo–O carbonate–tartrate and nitrate–tartrate gels, which is the critical stage of this preparation technique, is investigated in detail. X-ray diffraction, scanning electron microscopy, and ultraviolet–visible spectroscopy were used for the determination of crystal structure, surface morphology, and optical properties of the La–Mo–O: $x\text{Eu}_2\text{O}_3$  samples annealed at 400, 500, 600, 700, 800, 900, and 1,000 °C temperatures, respectively. The obtained results show that the thermal decomposition of the La–Mo–O tartrate gel precursors has occurred in a separate manner. The differences that came up during the thermal treatment of La–Mo–O tartrate gels have related only with the initial composition that determined the different crystallization ways of final compounds. Besides, the dopant concentration mainly influences the size of obtained particles and agglomeration of synthesized final materials. The initial composition of the La–Mo–O gel precursors has significant influence on the formation of final crystal phases at relatively lower temperatures than was expected according to the TG–DTA measurements. Finally, the optical properties of La–Mo–O tartrate gel precursors annealed at 500 °C

depend on the nature of the initial compounds, which were used during the aqueous sol–gel process.

**Keywords** Rare earth metals · Sol–gel processing · Thermal analysis · Optical properties

## Introduction

Rare earth molybdates with general formula  $\text{RE}_2\text{Mo}_3\text{O}_{12}$ , where RE is a trivalent cation, are found to be suitable hosts for transition metal and lanthanide ions and exhibit unusually high trivalent ion conduction [1]. This is the reason why these compounds are useful for many applications, such as luminescence centers due to the rapid development of diode lasers [2], solid oxide fuel cells (SOFC) [3], oxygen sensors, oxygen pumps, and catalysts for selective oxidation [4–10]. Most of these useful uses originate from electron transitions within the 4f shell and are highly sensitive to the compositions and structures of the rare earth compounds, especially the complexation state and the crystal field of the matrix in which the rare earth ions are coordinated [11].

Although the rare earth molybdates are important compounds for a wide range of applications, many different synthesis techniques for the preparation of such kind of materials are really desirable. For the most part, these materials are currently synthesized by solid-state reactions [12] with the mixtures of rare earth oxides and  $\text{MoO}_3$ . This process takes generally several days of heating with intermediate grindings. In this instance, high temperatures, lengthy heating process, and especially subsequent grinding damage the substance surfaces, resulting in the loss of expected of both physical and chemical properties. Besides, the volatility of  $\text{MoO}_3$  at elevated temperatures

R. Stankeviciute · A. Zalga (✉)  
Department of Applied Chemistry, Faculty of Chemistry, Vilnius University, Naugarduko Str. 24, 03225 Vilnius, Lithuania  
e-mail: arturas.zalga@chf.vu.lt

makes the synthesis of rare earth molybdates more difficult [1]. These limitations of the traditional solid-state method motivated us to explore the searching of synthesis technique that could shorten, facilitate, and reduce the preparation way of the rare earth molybdates.

In the past few decades, many researchers have carried out the studies on the formation of metal complexes with organic ligands. Furthermore, the metal complexes with organic ligands have been used for the preparation of ceramics and metal oxide thin films by a sol–gel process, using metal nitrates, chlorides, and acetates as starting materials. Besides, metal salts are very useful, inexpensive, and very easy to handle in comparison to metal alkoxides, and hence they are good alternatives for the conversion to oxides by thermal decomposition. They can be dissolved in many kinds of organic solvents in which metal complexes are formed. From this point of view, the wet synthesis route called an aqueous sol–gel method is really attractive and compared to other techniques, as it has the advantages of a good control of the starting materials and of the processing parameters, a high purity of the raw materials, and the low temperature of the process, which completely minimizes the volatility of molybdenum (VI) oxide by formation of double metal molybdates [13–17].

Although there is a lack of information using this method of synthesis, the resulting compound has the same structure as performing a solid-state synthesis. However, the properties that are exhibited by the tartaric acid-based synthesis product dramatically differ from the prevalent lanthanum molybdate ( $\text{La}_2\text{Mo}_3\text{O}_{12}$ ).

In this work, the aqueous sol–gel synthesis method was successfully used for the preparation of both the La–Mo–O carbonate–tartrate and nitrate–tartrate gel precursors with the initial composition for  $\text{La}_2\text{Mo}_3\text{O}_{12}$  ceramic, which were additionally calcined at 400, 500, 600, 700, 800, 900, and 1,000 °C temperatures. Moreover, the synthesis of the La–Mo–O tartrate gel precursors doped with  $x$  % of  $\text{Eu}_2\text{O}_3$  ( $x = 0, 0.5, 1.0, 2.0, 4.0,$  and  $8.0$ ) was also performed.

## Experimental

The synthesis of La–Mo–O tartrate gels with an initial composition of  $\text{La}_2\text{Mo}_3\text{O}_{12}$  prepared from the different starting compounds by an aqueous sol–gel synthesis route in the sol–gel process using tartaric acid as a complexing agent was carried out. The preparation data were placed according to the synthesis way in the Table 1. In addition, the doping of  $\text{Eu}_2\text{O}_3$  to the  $\text{La}_2\text{Mo}_3\text{O}_{12}$  ceramic was also performed. The lanthanum(III) carbonate hydrate ( $\text{La}_2(\text{CO}_3)_3 \cdot \text{H}_2\text{O}$ , 99.9 % AlfaAesar), lanthanum(III) nitrate hexahydrate ( $\text{La}(\text{NO}_3)_3 \cdot 6\text{H}_2\text{O}$ , 99.9 % AlfaAesar), ammonium molybdate (para) tetrahydrate ( $(\text{NH}_4)_6\text{Mo}_7\text{O}_{24} \cdot 4\text{H}_2\text{O}$ ,

**Table 1** Preparation data for the La–Mo–O tartrate gel precursors

Synthesis no.	Initial compounds	Complexing agent	Composition for final compound
1	$\text{La}_2(\text{CO}_3)_3, \text{MoO}_3$	Tartaric acid	$\text{La}_2\text{Mo}_3\text{O}_{12}$
2	$\text{La}(\text{NO}_3)_3 \cdot 6\text{H}_2\text{O}, (\text{NH}_4)_6\text{Mo}_7\text{O}_{24} \cdot 4\text{H}_2\text{O}$	Tartaric acid	$\text{La}_2\text{Mo}_3\text{O}_{12}$

99 % AlfaAesar), molybdenum(VI) oxide ( $\text{MoO}_3$ , 99.95 % AlfaAesar), and europium(III) oxide ( $\text{Eu}_2\text{O}_3$ , 99.99 % AlfaAesar) were used as starting materials and weighed according to the desired stoichiometric ratio. Nitric acid ( $\text{HNO}_3$ ), distilled water, and ammonia ( $\text{NH}_3 \cdot 4\text{H}_2\text{O}$ ) were used as solvents and reagents to regulate the pH of the solutions. Tartaric acid ( $\text{C}_4\text{H}_6\text{O}_6$ , 99.5 %) was used as a complexing agent. First, either molybdenum(VI) oxide or ammonium molybdate (para) tetrahydrate in distilled water was dissolved. In order to improve the solubility in distilled water of  $\text{MoO}_3$  especially, the concentrated ammonia solution was applied and stirred at 70–80 °C temperature. Then tartaric acid (TA), with molar ratios of  $\text{Mo}/\text{TA} = 0.25$ , was dissolved in a small amount of distilled water separately and added to the reaction mixture with continuous stirring at the same temperature. Next, after several hours the stoichiometric amount of lanthanum(III) carbonate hydrate, lanthanum(III) nitrate hexahydrate, and/or europium(III) oxide was mixed with the previous solution separately. To prevent the precipitation process, excess of ammonia was neutralized with concentrated  $\text{HNO}_3$ . Finally, the same amount of the aqueous solution of the complexing agent TA was repeatedly and separately added to the reaction mixture. The beaker with the solution was closed with a watch glass and left for 1 h with continuous stirring. The obtained clear solution was concentrated by slow evaporation at 80 °C in an open beaker. A yellow transparent gel has formed after nearly 90 % of the water evaporated under continuous stirring. After drying in an oven at 110 °C, fine-grained dark brown powders were obtained. Next to that, the La–Mo–O gel precursors were calcined for 5 h at 400, 500, 600, 700, 800, and 900 °C, respectively.

Thermal measurements were performed with TG–DTA, STA 6000 PerkinElmer instrument using a sample weight of about 10 mg and a heating rate of  $20 \text{ }^\circ\text{C min}^{-1}$  in flowing air ( $20 \text{ cm}^3 \text{ min}^{-1}$ ) at ambient pressure from room temperature to 1,000 °C. The residual powders that left after thermal treatment were additionally investigated by XRD analysis. X-ray diffraction (XRD) patterns were recorded in air at room temperature with a powder X-ray diffractometer Rigaku MiniFlex II using  $\text{Cu K}\alpha_1$  radiation. The spectra were recorded at the standard rate of  $1.5 \text{ } 2\theta/\text{min}^{-1}$ . The scanning electron microscopes (SEM)

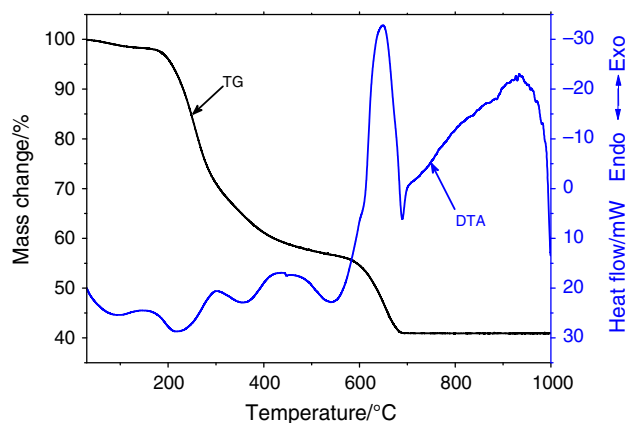


**Fig. 1** Combined TG-DTA curves of the La-Mo-O carbonate-tartrate precursor gel (synthesis 1) in flowing air

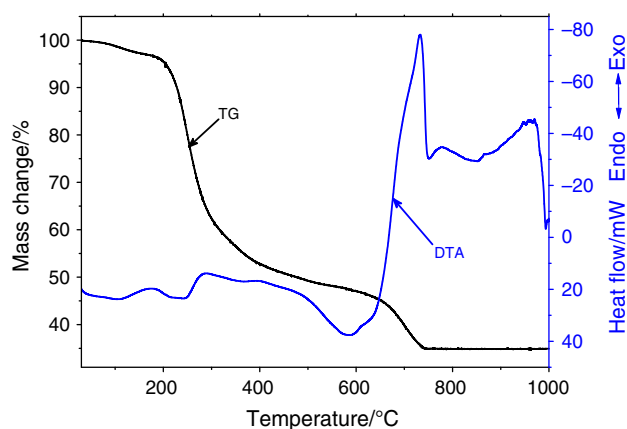


**Fig. 2** Combined TG-DTA curves of the La-Mo-O nitrate-tartrate precursor gel (synthesis 2) in flowing air

Hitachi TM3000 and Hitachi SU-70 were used to study the surface morphology and microstructure of the obtained ceramic samples. The reflection spectra were recorded at room temperature using a PerkinElmer Lambda 35 UV/Vis

spectrometer. The samples were well glued up on the flat substrate in order to form a thin layer on it and exited in 250–800 nm wavelength interval.

## Results and discussion

### Thermal analysis

The TG/DTA measurements of the La-Mo-O tartrate gel precursors that were carried out up to 1,000 °C at a heating rate of 20 °C min<sup>-1</sup> in flowing air (20 cm<sup>3</sup> min<sup>-1</sup>) at ambient pressure with a sample mass of about 10 mg in Figs. 1 and 2 are shown, respectively. According to the fact that both syntheses were performed in identical conditions, the differences that came into existence in TG/DTA curves have significant importance to the properties of final products. From this point of view, it is important to note that the thermal treatment of La-Mo-O tartrate gel precursors (Figs. 1, 2) also shows the different ability to absorb moisture from the air. In this case, the first mass loss of about 1 %, is shown in Fig. 1 and Table 2, with a range from 100 to 160 °C in temperature gives the conclusion that the humidity does not significantly affect the as-prepared La-Mo-O tartrate gel. In contrast to that, synthesis 2 (Fig. 2; Table 3) showed the mass loss up to 3 % of the gel precursor, which is closely related with both the absorption of moisture from air and residual water molecules in the sample after synthesis. This is the reason why the final mass loss of the synthesis 2 significantly differs from the case, presented in Table 2. The further increase of temperature from approximately 150–170 to 260–300 °C leads to the second endothermic effect and close after that to the exothermic process in the DTA curves that are related with the partial decomposition and rearrangement of organic compounds and initial salts in gel precursors. These processes have a similar manner in both cases and are concluded as decomposition of either metal nitrates or residue

**Table 2** Thermoanalytical data for the La-Mo-O carbonate-tartrate gel precursor (synthesis 1)

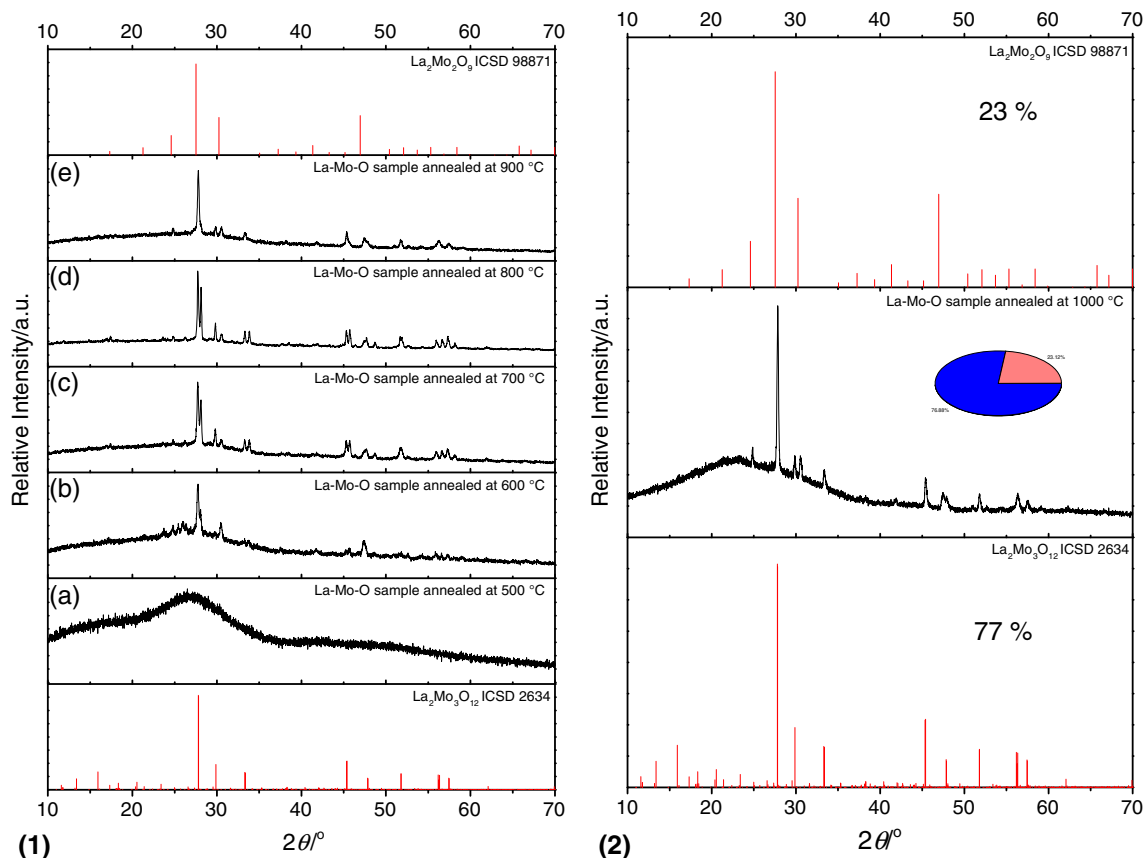
Range of temperature/°C	Mass			Heat			
	Change/%	Onset/°C	Residual/%	Flow/mJ	Onset/°C	End/°C	Enthalpy/J g <sup>-1</sup>
35–150	1.6	91.5	98.4	603.7	33.6	139.3	60.0
151–267	21.2	243.8	77.2	701.4	175.6	266.8	69.7
268–355	12.5	290.6	64.7	-451.0	269.4	345.9	-44.8
356–500	6.5	374.7	58.2	-966.8	377.3	457.5	-96.1
501–575	1.6	533.4	56.6	478.6	504.0	571.7	47.6
576–683	14.8	657.9	41.8	-6265.5	608.6	682.9	-622.9
684–800	0	-	41.8	697.3	684.1	694.0	69.3
801–906	0	-	41.8	64.4	803.0	902.6	6.4

**Table 3** Thermoanalytical data for the La–Mo–O nitrate–tartrate gel precursor (synthesis 2)

Range of temperature/°C	Mass			Heat			
	Change/%	Onset/°C	Residual/%	Flow/mJ	Onset/°C	End/°C	Enthalpy/J g <sup>-1</sup>
30–170	3.3	107.5	96.7	953.6	30.4	160.4	88.4
171–261	22.4	203.4	74.3	602.3	193.5	260.0	55.8
262–457	23.4	278.9	50.9	–1,612.1	262.2	360.0	–149.4
458–650	5.4	577.9	45.5	5,815.4	488.1	653.1	539.0
651–746	10.2	699.5	35.3	–9,129.9	660.3	745.5	–846.2
747–777	0	–	35.3	207.3	746.2	768.9	19.2
778–960	0	–	35.3	2736.5	792.5	955.1	253.6

of tartaric acid, or ammonia ions in the La–Mo–O gels. Next to that in the range of temperature from 260–300 to 460–520 °C, both the endothermic and exothermic behaviors with a mass loss of about 15–20 % on the TG/DTA curves with an exception of synthesis 2 have been observed. Sample 2, which presented thermoanalytical data in Table 2 shows mass loss of about 25 % that is related with the larger amount of tartrates that decompose up to 500 °C temperature. By further increasing the temperature from 500 to 600 °C, the crystallization of the final

compound started, which is clearly pronounced in both cases. The burning of elemental carbon, which formed during the decomposition of organic compounds under the thermal treatment initiated straight after that. The final mass loss of about 10–15 % and well-pronounced exothermic peaks from the 600 to 700 °C temperatures on the TG/DTA curves were observed in this range of temperature. The La–Mo–O nitrate–tartrate gel precursor (synthesis 2) fully decomposes until the mass remains constant only at 750 °C temperature that substantially separated

**Fig. 3** Standard ICSD cards of  $\text{La}_2\text{Mo}_3\text{O}_{12}$ ,  $\text{La}_2\text{Mo}_2\text{O}_9$ , and XRD patterns of the La–Mo–O carbonate–tartrate gel precursor (synthesis 1) annealed at 500, 600, 700, 800, 900, and 1,000 °C temperatures

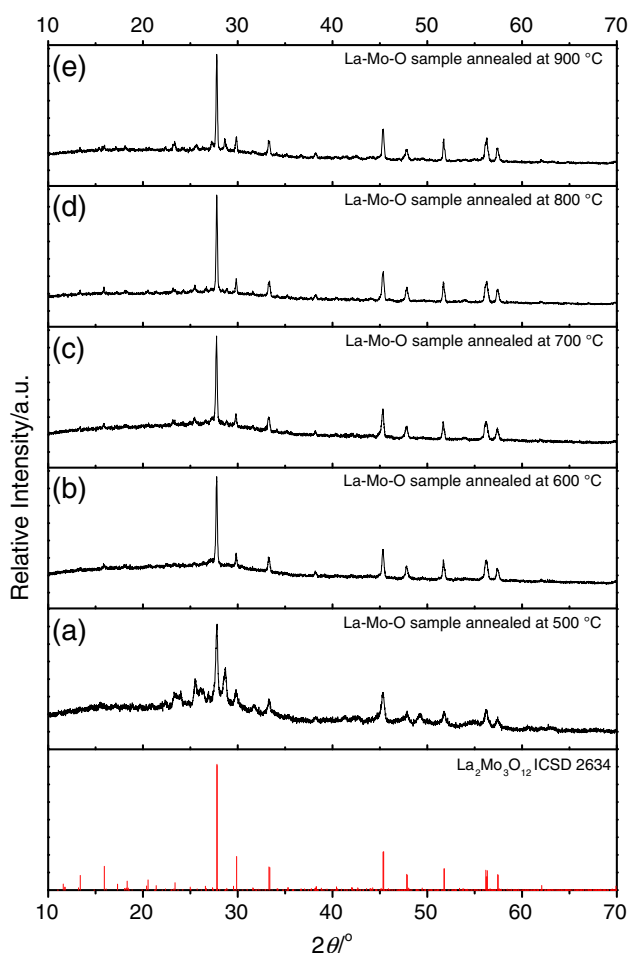


**Fig. 4** Standard ICSD card of  $\text{La}_2\text{Mo}_3\text{O}_{12}$  and XRD patterns of the La–Mo–O nitrate–tartrate gel precursor (synthesis 2) annealed at 500, 600, 700, 800, and 900 °C temperatures

from the other case. Moreover, the further crystallization processes of all samples up to 750 °C temperature on the DTA curves were also observed. It is interesting to note that the melting of the sample 2 presented in Fig. 2 from about 1,000 °C temperature has started. Meanwhile, sample 1 remained stable, which means that the melting point of this ceramic could be found at slightly higher temperature than 1,000 °C though strongly expressed endothermic behavior of the DTA curves has been observed. In conclusion, it is clear that the thermal decomposition of the La–Mo–O tartrate gel precursors has been in a separate manner. The differences that came up during the thermal treatment of La–Mo–O tartrate gels have related only with the initial composition that determined the different crystallization ways of final compounds.

#### X-ray diffraction

XRD patterns of La–Mo–O carbonate–tartrate gel precursor made by synthesis 1 and annealed at different temperatures

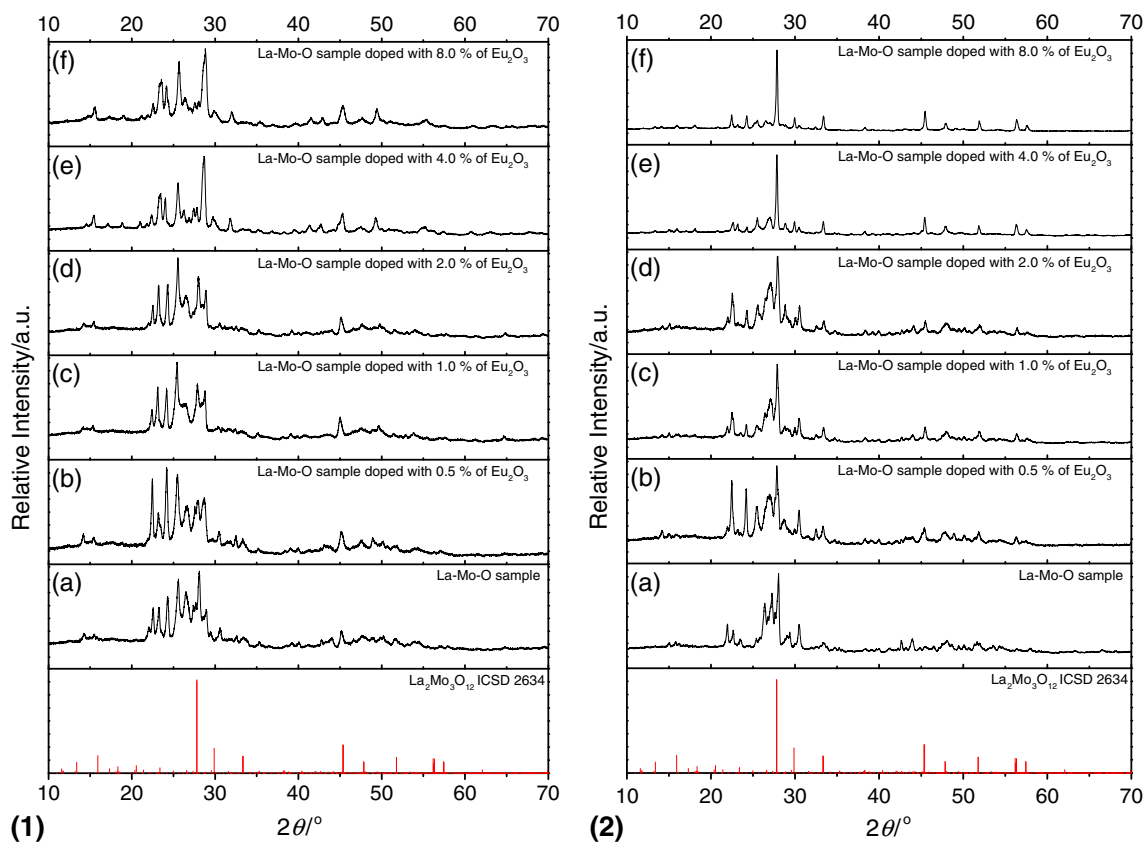
in the middle five panels of Fig. 3(1), are matched with the standard ICSD card of  $\text{La}_2\text{Mo}_3\text{O}_{12}$  and  $\text{La}_2\text{Mo}_2\text{O}_9$ , which are shown in the bottom and top panels. As seen in the XRD panel (a) of Fig. 3, increasing the sintering temperature to 500 °C causes no characteristic peaks to appear. This result is in good agreement with the data of the TG–DTA measurements (Fig. 1), which indicated the start of the last mass loss only at a temperature of 600 °C. By further increasing the temperature from 600 to 800 °C, the duplets of all characteristic peaks are attributed to the crystalline modifications of lanthanum molybdates ( $\text{La}_2\text{Mo}_3\text{O}_{12}$ ,  $\text{La}_6\text{Mo}_8\text{O}_{33}$ ,  $\text{La}_6\text{MoO}_{12}$ , and  $\text{La}_2\text{Mo}_2\text{O}_9$ ) with monoclinic and/or cubic crystal systems in cases b, c, and d. Next, the increase of temperature to 900 °C leads to the crystallization of the  $\text{La}_2\text{Mo}_3\text{O}_{12}$  phase (Fig. 3(1) case e), which consists of 95 % of all crystal phases identified from the top of XRD panel.

Figure 3(2) exhibits the XRD pattern of the La–Mo–O carbonate–tartrate gel precursor that was sintered from 30 to 1,000 °C at a heating rate of 20 °C  $\text{min}^{-1}$  in a thermal analyzer. From Fig. 3, it is clear that the increase of the annealing temperature to 1,000 °C does not enlarge the amount of  $\text{La}_2\text{Mo}_3\text{O}_{12}$  crystal phase in the final material. Therefore, the obtained results conclude that annealing length and sintering temperature are crucial factors, which influenced the formation of the  $\text{La}_2\text{Mo}_3\text{O}_{12}$  crystal phase in precursor made by synthesis 1.

Figure 4 exhibits XRD patterns of the La–Mo–O nitrate–tartrate gel precursor made by syntheses 2, which were obtained by sintering the dried gel for 5 h at 500, 600, 700, 800, and 900 °C temperatures in air atmosphere at ambient pressure. The sintering temperature of 500 °C is favorable for the formation of several crystal phases including monoclinic  $\text{La}_2\text{Mo}_3\text{O}_{12}$ . By further increasing the temperature to 600 °C (Fig. 4 panel b), the formation of characteristic peaks of the single-crystalline  $\text{La}_2\text{Mo}_3\text{O}_{12}$  compound in XRD patterns has started. No significant changes from XRD patterns in the samples sintered at 700, 800, and 900 °C temperatures in the La–Mo–O nitrate–tartrate gel precursor were observed.

Quite interesting XRD results were obtained from the La–Mo–O carbonate–tartrate and the La–Mo–O nitrate–tartrate gel precursors made by syntheses 1 and 2, respectively, and additionally doped with  $\text{Eu}_2\text{O}_3$  and annealed at 500 and 600 °C temperatures. Corresponding XRD patterns of these systems in Figs. 5 and 6 are displayed.

It is important to note that in the XRD patterns (Fig. 5) of the La–Mo–O carbonate–tartrate gel precursor made by synthesis 1, doped with europium oxide and annealed at 500 °C, several crystalline compounds like  $\text{MoO}_3$ ,  $\text{La}_2\text{Mo}_3\text{O}_{12}$ , and  $\text{La}_2\text{Mo}_2\text{O}_9$  were obtained. By increasing the sintering temperature to 600 °C and by the increase of dopant concentration to 8 % (Fig. 5(2) XRD panel f) most



**Fig. 5** Standard ICSD card of La<sub>2</sub>Mo<sub>3</sub>O<sub>12</sub> and XRD patterns of La–Mo–O carbonate–tartrate gel precursor (synthesis 1) doped with  $x$  % Eu<sub>2</sub>O<sub>3</sub> and annealed at 500 (1) and 600 °C (2) temperatures

characteristic peaks of side phases tended to disappear and only the formation of La<sub>2</sub>Mo<sub>3</sub>O<sub>12</sub> crystal phase has started. In conclusion, from the XRD patterns, it is clear that La–Mo–O samples made by synthesis 1 and doped by  $x$  % of Eu<sub>2</sub>O<sub>3</sub> contain a significant amount of MoO<sub>3</sub> that is ready to react with europium oxide by increasing of annealing temperature to 600 °C.

Quite a different view of XRD patterns (Fig. 6) compared with previous case in Eu–La–Mo–O nitrate–tartrate system is shown. In this case, the formation of the La<sub>2</sub>Mo<sub>3</sub>O<sub>12</sub> crystal phase has started above 500 °C. By increasing the sintering temperature to 600 °C (Fig. 6(2)) only single-crystalline La<sub>2</sub>Mo<sub>3</sub>O<sub>12</sub> compound has formed and no characteristic peaks attributable to the phase has been observed. It should also be noted that by increasing the dopant concentration, the width of the characteristic peaks of the La<sub>2</sub>Mo<sub>3</sub>O<sub>12</sub> in Fig. 6(2) tends to increase, which suggests the formation of smaller crystallites than in the case without doping.

#### SEM micrographs

To understand the crystal growth of the final products, we investigated the influence of the temperature, dopant

concentration, and initial compounds on the morphology of the La–Mo–O gel precursors.

The SEM micrographs of the La–Mo–O sample made by synthesis 1 and annealed at 400, 600, and 700 °C are shown in Fig. 7. The surface of the La–Mo–O carbonate–tartrate gel precursor annealed at 400 °C consists of many irregular particles that vary in size from 500 nm to 5 μm. It is interesting to note that the grains larger than 1 μm from the spherical particles less than 500 nm in size are composed. As shown in Fig. 7b, by increasing the sintering temperature to 600 °C the surface morphology of the analyzed sample was changed completely by thermal decomposition and melting of the smaller spherical particles and composing of the porous irregular particles with size up to 10 μm. This result is in good agreement with TG/DTA data presented in Fig. 1 and Table 2, which indicated the mass loss of about 15 % in the range of temperature from 575 to 683 °C. By further increasing the annealing temperature to 700 °C, there is an initial transformation of porous irregular particles to both the spherical particles and conglomerates with sizes of about 1–5 μm by estimate.

The surface view of SEM micrographs of the annealed La–Mo–O nitrate–tartrate gel precursor at 400, 600, and

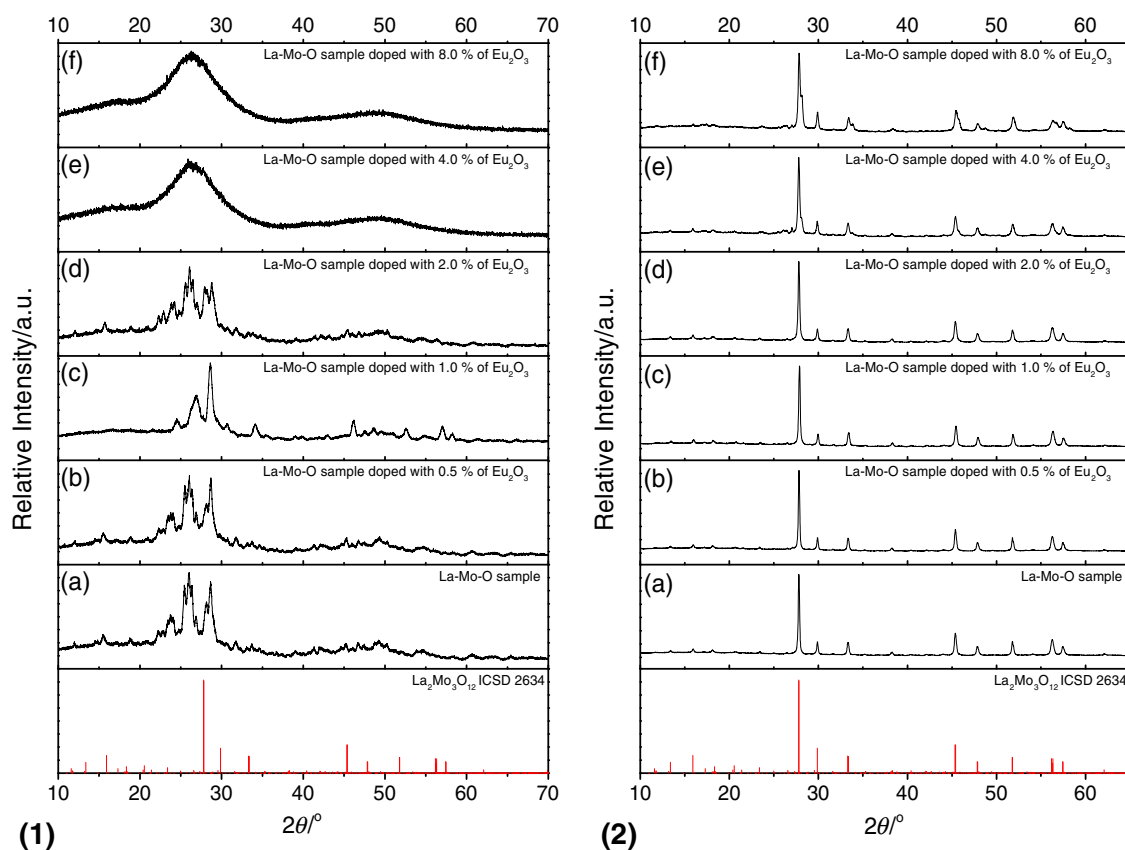


**Fig. 6** Standard ICSD card of  $\text{La}_2\text{Mo}_3\text{O}_{12}$  and XRD patterns of La–Mo–O nitrate–tartrate gel precursor (synthesis 2) doped with  $x$  %  $\text{Eu}_2\text{O}_3$  and annealed at 500 (1) and 600 °C (2) temperatures

700 °C (Fig. 8) was completely different comparing with the previous case presented in Fig. 7, respectively. In this case, the surface morphology of the sample sintered at 400 °C is composed from the plate-like crystals that vary in size from several micrometers to 20  $\mu\text{m}$ . This result is in agreement with the conclusions made from the XRD patterns, which are presented in Fig. 4. By increasing the sintering temperature to 600 °C (Fig. 8b), the surface of regular crystals became porous and rough because of the decomposition of elemental carbon in the gel precursor. Finally, by the further increase of temperature to 700 °C, the porous surface structure of investigated samples tends to increase, from which we can conclude the further crystallization of crystalline compounds.

In Figs. 9 and 10, the effect of dopant concentration on the surface morphology of the La–Mo–O tartrate gel precursors by SEM was investigated in detail. The SEM micrographs of the La–Mo–O carbonate–tartrate gel prepared by synthesis 1, doped with  $x$  % of  $\text{Eu}_2\text{O}_3$  (where,  $x = 0, 1, 2, 4$  and 8) and annealed at 500 °C for 5 h in air in Fig. 9 are shown. As seen from Fig. 9a in the sample, the agglomerates with size of about 10  $\mu\text{m}$  have formed. The surface of these irregular particles consists of

elongated continuous rounded particles with sizes from 100 nm to 1  $\mu\text{m}$  as shown in the right top corner of Fig. 9a. The addition of 0.5 %  $\text{Eu}_2\text{O}_3$  to the La–Mo–O carbonate–tartrate gel precursor (Fig. 9b) leads to the formation of a porous structure. The pores with a size of about 1  $\mu\text{m}$  are composed from spherical particles that vary in size from 100 to 200 nm as presented in the right top corner of Fig. 9b. By further increasing the dopant concentration, the surface morphology of the prepared La–Mo–O gel precursor significantly changed. The porous structure observed in the previous case disappeared and the agglomerates of elongated particles with sizes from 100 to 500 nm as shown in the right top corner of Fig. 9c have formed. The surface morphology of the La–Mo–O carbonate–tartrate gel precursor doped with 2 %  $\text{Eu}_2\text{O}_3$  (Fig. 9d) is similar to that which is presented in Fig. 9a. In this case, the particles are slightly larger and composed in a more compact way. By further increase of the dopant concentration in the La–Mo–O sample (Fig. 9e), leads to the formation of irregular crystals that vary in size from 5 to 20  $\mu\text{m}$ . Besides, the agglomerates composed of the spherical particles, which vary in size from 50 to 150 nm, surround these crystals, as shown in the right top corner of

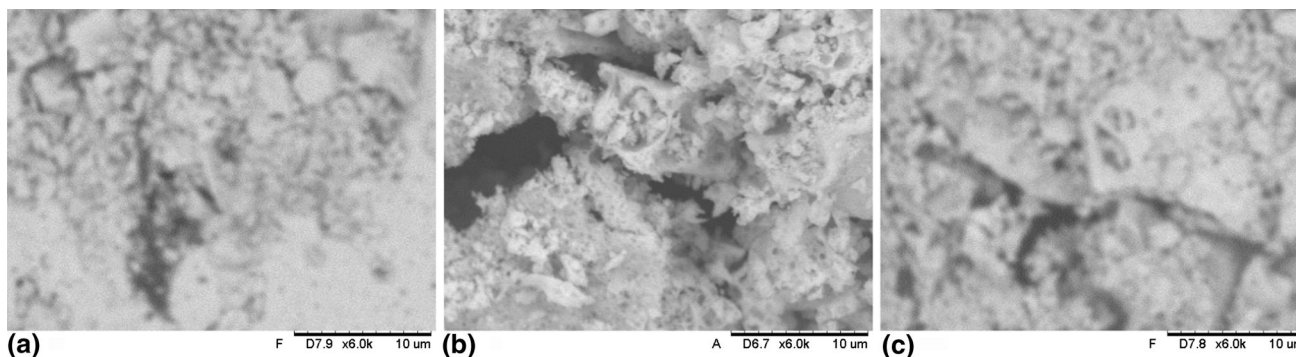


**Fig. 7** SEM micrographs of La–Mo–O carbonate–tartrate precursor gel (synthesis 1) annealed at **a** 400 °C, **b** 600 °C, and **c** 700 °C temperatures

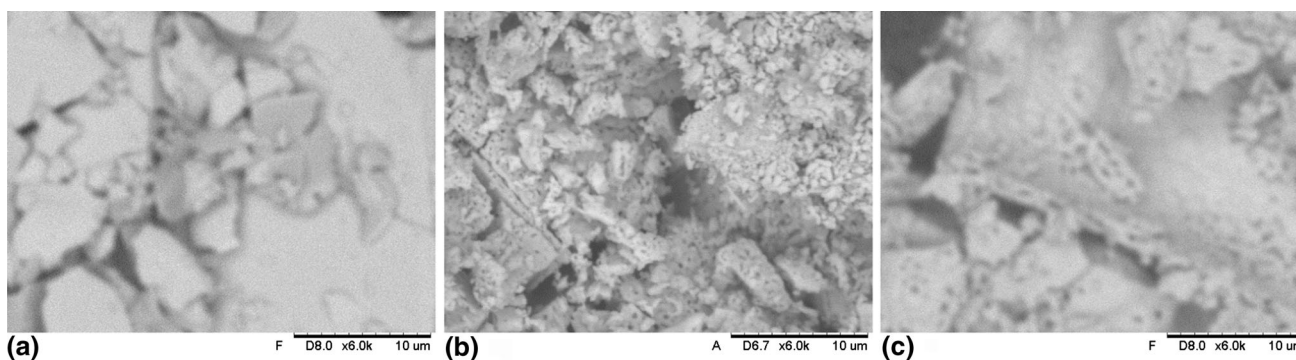


**Fig. 8** SEM micrographs of La–Mo–O nitrate–tartrate precursor gel (synthesis 2) annealed at **a** 400 °C, **b** 600 °C, and **c** 700 °C temperatures

Fig. 9e. Meanwhile, the surface morphology of the La–Mo–O carbonate–tartrate gel precursor doped with 8 %  $\text{Eu}_2\text{O}_3$  (Fig. 9f) only slightly differs from the case presented in Fig. 9e. In this SEM micrograph, the agglomerates of spherical particles with sizes of about several micrometers surround the irregular crystals. The surface of these irregular crystals was composed from the close-packed melted particles with sizes less than 1  $\mu\text{m}$ .

The corresponding SEM micrographs of the La–Mo–O nitrate–tartrate gel precursor made by synthesis 2, doped with  $x$  % of  $\text{Eu}_2\text{O}_3$  (where  $x = 0, 1, 2, 4,$  and  $8$ ) and annealed at 500 °C for 5 h in air are presented in Fig. 10. As seen from Fig. 10a, in the La–Mo–O nitrate–tartrate gel the irregular crystals with sizes from 1 to 10  $\mu\text{m}$  have formed. The surface morphology of these crystals was composed from the close-packed melted spherical particles with sizes of about 100 nm, which form the spherical holes with diameters of one micrometer, as shown in the top right corner of Fig. 10a. The addition of 0.5 %  $\text{Eu}_2\text{O}_3$  to the La–Mo–O nitrate–tartrate gel precursor (Fig. 10b) leads to the formation of irregular crystals with sizes from 5 to 20  $\mu\text{m}$ , which composed from the close-packed melted spherical particles with sizes less than 100 nm as presented in the top right corner of Fig. 10b. By further increasing the concentration of  $\text{Eu}_2\text{O}_3$  in the La–Mo–O sample, the porous

structure with pores less than 100 nm in diameter as shown in the top right corner of Fig. 10c was observed. The surface morphology of the La–Mo–O nitrate–tartrate gel precursor doped with 2 %  $\text{Eu}_2\text{O}_3$  in Fig. 10d showed that the irregular crystals with diameters larger than 2  $\mu\text{m}$  were formed. In this case, the crystals were composed from the irregular spherical particles that vary in size from 100 to 500 nm as presented in the right corner of Fig. 10d. Meanwhile, the surface morphology of the La–Mo–O nitrate–tartrate gel precursors doped with 4 and 8 % of  $\text{Eu}_2\text{O}_3$  (Fig. 10e, f) is composed from the particles with sizes less than 50 nm, the spherical forms of which are not well pronounced, as presented in the top right corners of Fig. 10e, f. Moreover, the surfaces of both samples have uneven areas, which are attributed to the unreacted amorphous parts of the La–Mo–O nitrate–tartrate samples. It is also important to note that these obtained results are in good agreement with the data collected from the XRD patterns presented in Fig. 6.

In conclusion, it should be noted that the temperature, dopant concentration, initial composition, and different initial compounds have significant influence to the formation on the surface morphology of the final materials. From this point of view, the temperature determines both the thermal decomposition and crystal growth of the La–Mo–O



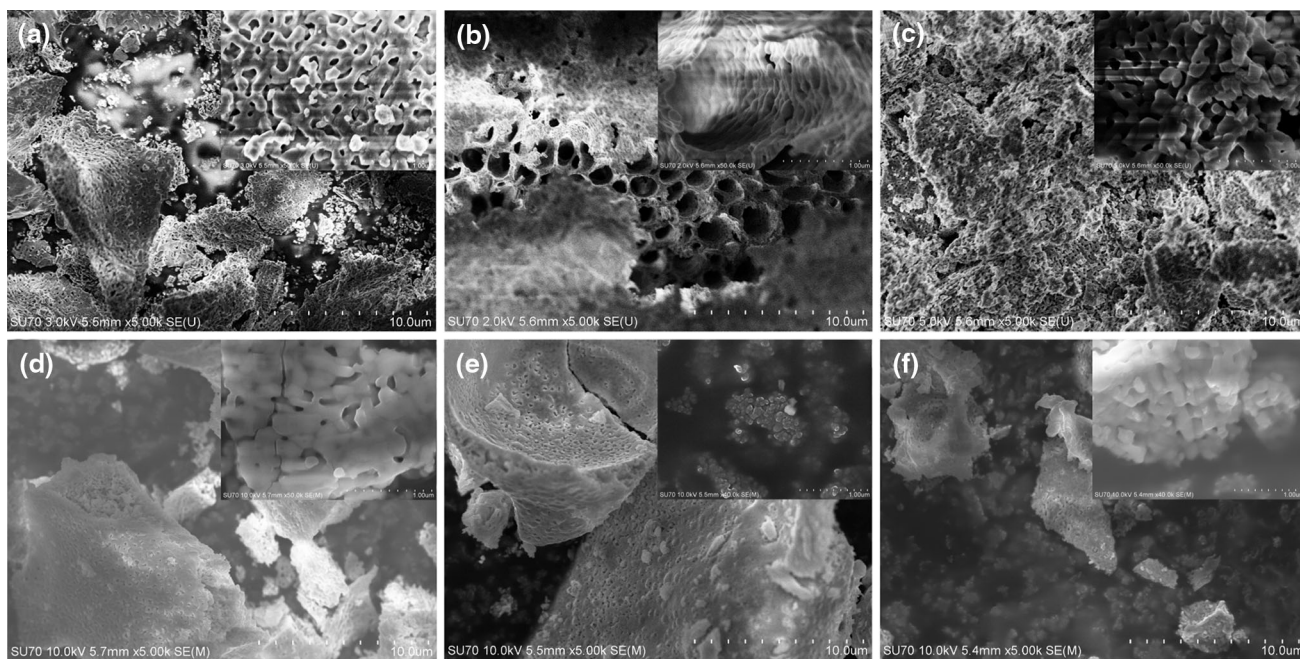


**Fig. 9** SEM micrographs of La–Mo–O carbonate–tartrate precursor gel (synthesis 1) doped with 0 %  $\text{Eu}_2\text{O}_3$  (a), 0.5 %  $\text{Eu}_2\text{O}_3$  (b), 1 %  $\text{Eu}_2\text{O}_3$  (c), 2 %  $\text{Eu}_2\text{O}_3$  (d), 4 %  $\text{Eu}_2\text{O}_3$  (e), 8 %  $\text{Eu}_2\text{O}_3$  (f) and annealed at 500 °C temperature

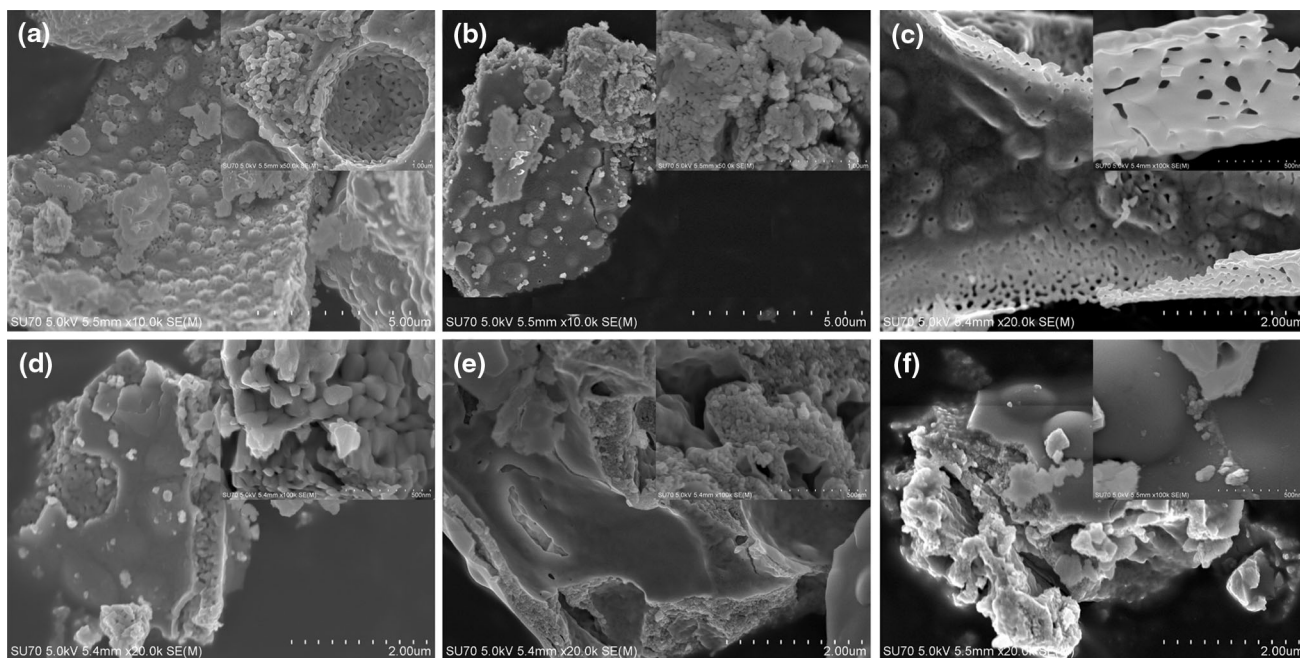


**Fig. 10** SEM micrographs of La–Mo–O nitrate–tartrate precursor gel (synthesis 4) doped with 0 %  $\text{Eu}_2\text{O}_3$  (a), 0.5 %  $\text{Eu}_2\text{O}_3$  (b), 1 %  $\text{Eu}_2\text{O}_3$  (c), 2 %  $\text{Eu}_2\text{O}_3$  (d), 4 %  $\text{Eu}_2\text{O}_3$  (e), 8 %  $\text{Eu}_2\text{O}_3$  (f) and annealed at 500 °C temperature

gel precursors. Meanwhile, the dopant concentration mainly influences the size of obtained particles and agglomeration of synthesized final materials. Besides, the initial composition of the La–Mo–O gel precursors has significant influence on the formation of final crystal phases at relatively lower temperatures than was expected

according to the TG/DTA measurements. Finally, the different initial compounds, which are well presented in the Table 1, mostly determine the different way of thermal decomposition processes that usually occurred because of different intermediate products, which formed during the sol–gel processing.

**Fig. 11** UV–Vis reflectance spectra of La–Mo–O carbonate–tartrate gel precursors (synthesis 1) doped with  $x$  %  $\text{Eu}_2\text{O}_3$  and annealed at 500 °C temperature

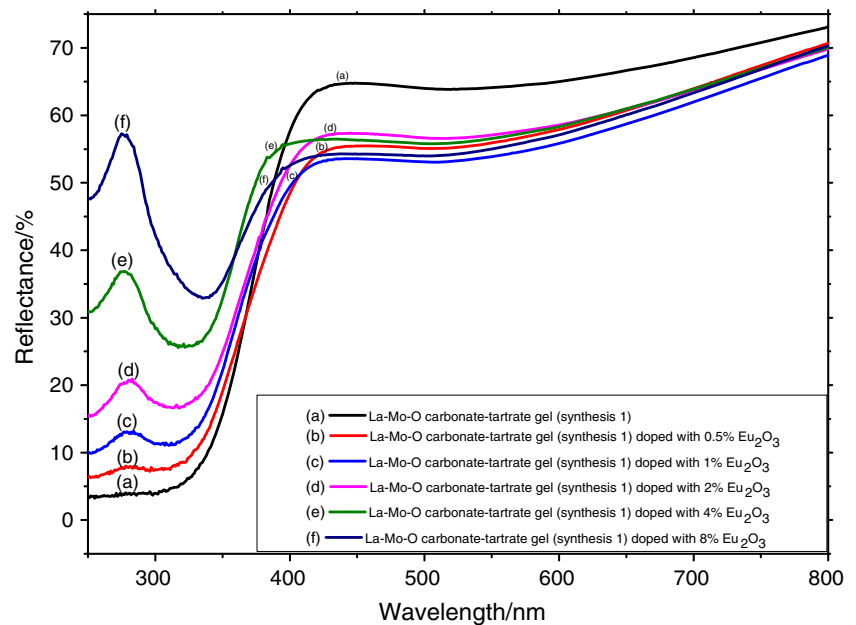
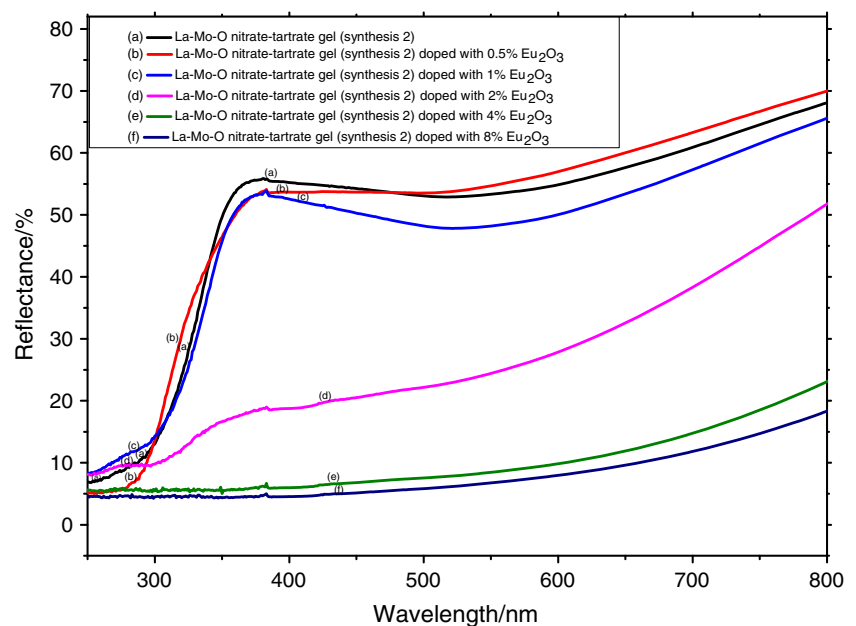


**Fig. 12** UV–Vis reflectance spectra of La–Mo–O nitrate–tartrate gel precursors (synthesis 2) doped with  $x$  %  $\text{Eu}_2\text{O}_3$  and annealed at 500 °C temperature



### Reflection measurements

The optical properties of the La–Mo–O tartrate gel precursors doped with europium(III) oxide were also investigated. The UV–Vis reflectance spectra of La–Mo–O tartrate gel precursors prepared by syntheses 1 and 2, doped with  $x$  % of  $\text{Eu}_2\text{O}_3$  ( $x = 0, 0.5, 1, 2, 4$ , and 8) and annealed at 500 °C are shown in Figs. 11 and 12. As seen from Fig. 11, the nature of the reflectance spectra of La–Eu–Mo–O carbonate–tartrate samples strongly depends on the amount of europium oxide inserted into the La–Mo–O ceramic. It is clear that in the range of wavelength from 800 to 400 nm, the reflectance of analyzed samples is more

or less stable and slightly varies beside 60 %. By further decreasing the wavelength from 400 to 250 nm, the reflectance tends to decrease significantly to 4 % in the case of La–Mo–O sample without doping. Meanwhile, in the case of La–Mo–O carbonate–tartrate samples doped with  $\text{Eu}_2\text{O}_3$ , the well-defined reflection band in the range of 350–250 nm is observed. The maximum of this band has the top value of 57.3 % in the La–Mo–O carbonate–tartrate gel precursor doped with 8 % of europium oxide. It is also interesting to note that no characteristic peaks attributable to the reflectance of  $\text{Eu}^{3+}$  ions in the La–Mo–O host-lattice were observed. According to the results presented in [17],  $\text{MoO}_4^{2-}$  group exhibited a very broad asymmetric reflection

in the range of 180–300 nm, this reflection band to oxygen to molybdenum (O → Mo) ligand-to-metal charge transfer in the  $\text{MoO}_4^{2-}$  group exhibited by  $\text{Eu}_2\text{O}_3$  was attributed.

Completely different results from the reflectance spectra, presented in Fig. 12, by combustion at 500 °C of the La–Mo–O nitrate–tartrate gel precursor made by synthesis 2 and doped with  $x$  % of  $\text{Eu}_2\text{O}_3$  ( $x = 0, 0.5, 1, 2, 4, \text{ and } 8$ ) were obtained. In this case, the addition of europium oxide to the La–Mo–O ceramic significantly decreased the reflectance of obtained sample even in the range of wavelength from 800 to 400 nm. In addition, the reflection band of the La–Eu–Mo–O nitrate–tartrate samples, annealed at 500 °C located between 315 and 250 nm, corresponding to oxygen to molybdenum (O → Mo) ligand-to-metal charge transfer in the  $\text{MoO}_4^{2-}$  group were not observed. In conclusion, it is clear that the “optical properties of La–Mo–O tartrate gel precursors annealed at 500 °C of temperature depend significantly on the nature of the initial compounds, which were used during the aqueous sol–gel process.

## Conclusions

Summarizing results obtained from the TG–DTA, XRD, SEM, and UV–Vis measurements it can be concluded that aqueous sol–gel synthesis method is a suitable technique for the preparation of the single-phase  $\text{La}_2\text{Mo}_3\text{O}_{12}$  at a relatively low temperature of 600 °C. The thermal decomposition of the as-prepared La–Mo–O tartrate gel precursors clearly showed that the differences that came up during the thermal treatment of the samples are closely related with the nature of the initial compounds. Despite the fact that the La–Mo–O nitrate–tartrate gel precursor fully decomposes until the mass remains constant only at 750 °C, the formation of several crystal phases including monoclinic  $\text{La}_2\text{Mo}_3\text{O}_{12}$  before 500 °C has started. Moreover, it was also shown that the temperature, dopant concentration, and different initial compounds have significant influence to the formation on both the surface morphology and the optical properties of the final materials. In this case, the dopant concentration mainly influences the size of the obtained particles and agglomeration of synthesized final materials. Meanwhile, the initial composition of the La–Mo–O gel precursors has significant influence on the formation of final crystal phases at relatively lower temperatures than was expected according to the TG/DTA measurements. Besides, the optical properties of La–Mo–O tartrate gel precursors annealed at 500 °C depend significantly on the nature of the initial compounds, which were used during the aqueous sol–gel process.

**Acknowledgements** The study was funded from the European Community’s social foundation under Grant Agreement No. VPI-3.1-ŠMM-08-K-01-004/KS-120000-1756.

## References

- Liang EJ, Huo HL, Wang Z, Chao MJ, Wang JP. Rapid synthesis of  $\text{A}_2(\text{MoO}_4)_3$  ( $\text{A} = \text{Y}^{3+}$  and  $\text{La}^{3+}$ ) with a  $\text{CO}_2$  laser. *Solid State Sci.* 2009;11:139–43.
- Forster PL, Lugao AB, Brito HF, Parra DF. Calorimetric investigations of luminescent films polycarbonate (PC) doped with europium complex  $[\text{Eu}(\text{TAA})_3(\text{H}_2\text{O})_2]$ . *J Therm Anal Calorim.* 2009;97:497–502.
- Hutchinson TP, Radosavljević Evans I. Comment on new oxide ion conductors  $\text{La}_3\text{MMo}_2\text{O}_{12}$  ( $\text{M} = \text{In, Ga, Al}$ ). *Solid State Ion.* 2008;178:1660–2.
- Zhang GG, Fang QF, Wang XP, Yi ZG. AC impedance and dielectric relaxation study on the effects of the excess Pb introduced in  $\text{La}_2\text{Mo}_2\text{O}_9$  oxide-ion conductors. *Phys Status Sol.* 2003;199:329–34.
- Marrero-Lopez D, Canales-Vazquez J, Zhou W, Irvine JTS, Nunez P. Structural studies on  $\text{W}^{6+}$  and  $\text{Nd}^{3+}$  substituted  $\text{La}_2\text{Mo}_2\text{O}_9$  materials. *J Solid State Chem.* 2006;179:278–88.
- Ren F, Chen D. A novel red-emitting phosphor for white light-emitting diodes. *J Alloy Compd.* 2010;499:53–6.
- Chen Z, Bu W, Zhang N, Shi J. Controlled construction of monodisperse  $\text{La}_2(\text{MoO}_4)_3\text{:Yb, Tm}$  microarchitectures with up-conversion luminescent property. *J Phys Chem C.* 2008;112:4378–83.
- Ding Y, Li C, Guo R. Facile fabrication of pompon like microarchitectures of lanthanum molybdate via an ultrasound route. *Ultrason Sonochem.* 2010;17:46–54.
- Huang X, Wang G. Growth and optical characteristics of  $\text{Er}^{3+}$ :  $\text{LiLa}(\text{MoO}_4)_2$  crystal. *J Alloy Compd.* 2009;475:693–7.
- Filipek E, Rychlowska-Himmel I, Paczesna A. Thermal stability of  $\text{In}_2(\text{MoO}_4)_3$  and phase equilibria in the  $\text{MoO}_3$ – $\text{In}_2\text{O}_3$  system. *J Therm Anal Calorim.* 2012;109:711–6.
- Zhang N, Bu W, Xu Y, Jiang D, Shi J. Self-assembled flowerlike europium-doped lanthanide molybdate microarchitectures and their photoluminescence properties. *J Phys Chem C.* 2007;111:5014–9.
- Mhadhbi N, Corbel G, Lacorre P, Bulou A. Partial substitution of  $\text{Mo}^{6+}$  by  $\text{S}^{6+}$  in the fast oxide ion conductor  $\text{La}_2\text{Mo}_2\text{O}_9$ : synthesis, structure and sulfur depletion. *J Solid State Chem.* 2012;190:246–56.
- Guo C, Chen T, Luan L, Zhang W, Huang D. Luminescent properties of  $\text{R}_2(\text{MoO}_4)_3\text{:Eu}^{3+}$  ( $\text{R} = \text{La, Y, Gd}$ ) phosphors prepared by sol–gel process. *J Phys Chem Solids.* 2008;69:1905–11.
- Tönsuaadu K, Zalga A, Beganskiene A, Kareiva A. Thermoanalytical study of the YSZ precursors prepared by aqueous sol–gel synthesis route. *J Therm Anal Calorim.* 2012;110:77–83.
- Zalga A, Moravec Z, Pinkas J, Kareiva A. On the sol–gel preparation of different tungstates and molybdates. *J Therm Anal Calorim.* 2011;105:3–11.
- Braziulis G, Stankeviciute R, Zalga A. Sol-gel derived europium doped  $\text{CaMoO}_4\text{:Eu}^{3+}$  with complex microstructural and optical properties. *Mater Sci Medzg.* 2014;20:90–6.
- Braziulis G, Janulevicius G, Stankeviciute R, Zalga A. Aqueous sol–gel synthesis and thermoanalytical study of the alkaline earth molybdate precursors. *Therm Anal Calorim.* 2013;. doi:10.1007/s10973-013-3579-0.